

Recognition and transport of natural and synthetic siderophores by microbes

KENNETH N. RAYMOND

Department of Chemistry
University of California
Berkeley, CA 94720, USA

Iron transport represents a unique problem in biology. In general, organisms have large requirements for iron, creating a need for both transport and storage systems. For aerobic organisms this means that ferric ion, which is completely insoluble as the hydroxide at neutral pH, must be complexed so that it can be solubilized for both mobilization and storage. For bacteria this problem is particularly acute since they must obtain their iron from a hostile environment where the available concentrations of $[\text{Fe}^{3+}]$ correspond to equilibrium concentrations lower than 10^{-18} molar. To accomplish this microorganisms synthesize low-molecular-weight sequestering agents, siderophores, that are extraordinarily stable iron complexing agents. This paper gives an overview of the iron complexation, mobilization, and cellular transport of iron by siderophores. Particular focus is on the tri-catechol siderophore enterobactin (produced by *Escherichia coli*), its mobilization of iron, and the relationship of the virulence of pathogenic microorganisms to their acquisition of iron utilizing siderophores. The recent crystal structure determination of enterobactin and the synthesis of unusually stable analogs provide a basis for understanding the unique stability, structure and function of this remarkable molecule.

INTRODUCTION

Although it can be said that the first siderophore (mycobactin) was isolated as early as 1912 (ref. 1) it was nearly half a century later that mycobactins, and subsequently other siderophores, were characterized as low-molecular weight ferric ion chelating agents that are produced specifically by microorganisms in order to solubilize and take up iron (ref. 2, 3). Since iron is absolutely required by all except a few microorganisms, and is certainly required by all pathogenic bacteria, understanding the uptake of iron by siderophores and the regulation of this process has been a significant problem in an area of biochemistry that includes portions of bioorganic and bioinorganic chemistry (ref. 4, 5). In recent years the medical significance of siderophore mediated iron transport has increased as our understanding of the role of iron in several disease states has increased. The toxicity of iron when present in excess, as occurs with β thalassemia major (Cooley's anemia), is well documented and will not be further reviewed here (ref. 6, 7, 8, 9, 10). The role of iron in tissue damage following a heart attack has more recently been characterized. Approaches to minimizing tissue damage following a heart attack, using ferric ion sequestering agents, are being explored in a number of laboratories around the world (ref. 11, 12). More significant for this presentation, it has become very clear that iron plays a key role in the pathogenicity of many (perhaps most) diseases caused by bacterial infections. The number one killer of children in the world, infantile enteritis, is one example (ref. 13, 14). Cholera (ref. 15), leprosy (ref. 16), and tuberculosis (ref. 17), are other examples. The latter is of particular concern, as new bacterial strains have caused tuberculosis to be on the increase in developed nations of the world.

Our research has focused on the coordination chemistry aspects of siderophore-mediated transport. As shown in Figure 1, the substitution of Fe^{3+} by Cr^{3+} gives a molecule that is unchanged in geometry but quite different in its ligand exchange properties and optical spectra. This represented the first use of a kinetically inert siderophore metal complex (ref. 18, 19). All of the siderophores (ref. 4) incorporate iron in the +3 oxidation state and in the high spin form. With five unpaired electrons there are no ligand field (d to d-orbital) allowed transitions and there is no ligand field stabilization of the complex with respect to ligand exchange or isomerization processes.

Nevertheless, the iron complexes are intensely colored because of charge transfer processes that have only recently been understood (ref. 20). In contrast, the chromic complexes have very well characterized d to d-orbital transitions that generate the characteristic VIS/UV and circular dichroism spectra shown in Figure 1. Furthermore, the extreme kinetic inertness of the chromic complexes allows the use of these metal-substituted siderophore complexes as probes of siderophore mediated

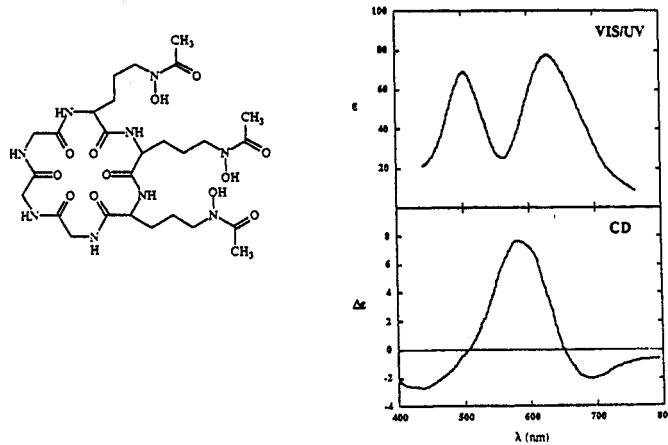
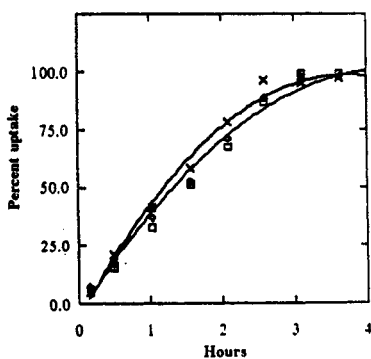


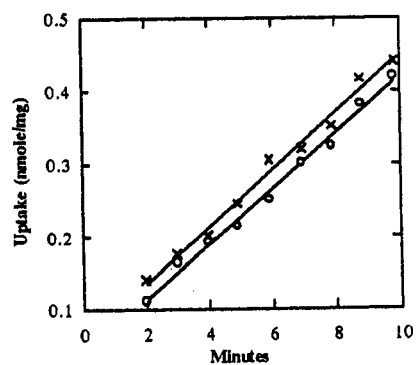
Fig. 1. The first synthesis of a kinetically inert siderophore complex. The VIS/UV and CD spectra of the chromic complex of desferriferrichrome is shown. This established the Λ cis coordination environment of the metal center in this complex (ref. 18).

iron uptake. Shown in Figure 1 is the siderophore produced by *Ustilago sphaerogena*, ferrichrome, one of the first siderophores or family of siderophores characterized. In Figure 2 is shown an example of the use of the chromic ferrichrome complex in probing siderophore mediated iron uptake. Using a radioactive label for the natural iron ferrichrome complex, the rate of uptake of the iron could be monitored as shown in Figure 2. However, since in principle this complex could be labile, it was not known whether the ligand was accompanying the iron uptake. The observation that the chromic-substituted complex was taken up at the same rate (observed under a microscope the microorganism can be seen to turn green!) constituted the first example of a kinetically-inert complex used to probe siderophore mediated iron uptake. The result of this and similar experiments (ref. 4) has established a general pattern: that iron uptake mediated by siderophores normally involves direct transport of the metal complex via active transport processes that utilize proteins imbedded in the outer membrane. These proteins recognize particular features of the siderophore complex and are highly sensitive to the geometry at the metal center, as will be shown.



Uptake of ferrichrome (X) and Λ -chromic $[^{14}\text{C}]$ -desferriferrichrome ($[^{14}\text{C}]$; \square ; Δ) by *U. sphaerogena*.

Fig. 2. The uptake of the natural Fe^{3+} and kinetically inert Cr^{3+} complexes of ferrichrome in the microorganism *Ustilago sphaerogena* (ref. 19).



Uptake of $[^{67}\text{Ga}]$ ferrioxamine B (X) and $[^{55}\text{Fe}]$ ferrioxamine (O), $5 \mu\text{M}$ concentration.

Fig. 3. The use of Ga^{3+} substitution for Fe^{3+} to probe the role of reduction in siderophore-mediated microbial iron transport (ref. 22).

Figure 3 illustrates another example of metal ion substitution. Since iron release from these powerful complexing agents is an essential portion of the transport process, one important question is whether a redox process is a determinant in the overall kinetics of iron uptake. Early on it was suggested that Ga^{3+} , a very close structural analog to high spin Fe^{3+} , could be used for this purpose. Since gallium has no stable +2 oxidation state, any process that requires reduction of Fe^{3+} to Fe^{2+} would show very different behavior when gallium is substituted in place of iron. In a key early experiment Tom Emery and coworkers (ref. 21) examined this issue. A more extensive examination of the role of a redox process in the rate of iron uptake mediated by ferrioxamine B into *Streptomyces pilosus* showed that the metal ion uptake rate was the same whether the gallium complex or the ferric complex was used (ref. 22). This showed that the kinetics of the transport process did not involve reduction. Iron release via reduction is a later event that follows the active transport of the complex into the cell.

The use of the optical spectra of siderophore complexes to predict coordination geometry or chirality was first accomplished in the case of enterobactin (ref. 23) (Figure 4). Again, substitution of Fe^{3+} by Cr^{3+} gives a characteristic absorption spectra. In the case of the VIS/UV spectrum (upper panel in Figure 4) the individual ligand field transitions do not show up clearly because of the strong charge transfer tail in the near UV. In contrast, the circular dichroism spectrum (lower panel) is very clean and, compared to the corresponding chromic ferrichrome complex, clearly shows that the metal center in enterobactin has an opposite chirality to that of the metal center in ferrichrome. Since the crystal structure of ferrichrome A had been determined and the absolute configuration was known to be Λ , this established the chirality of the metal center in enterobactin as Δ . The metal complex of enterobactin is a diastereoisomer, since the chirality of the ligand is imposed by its formation from three serine molecules.

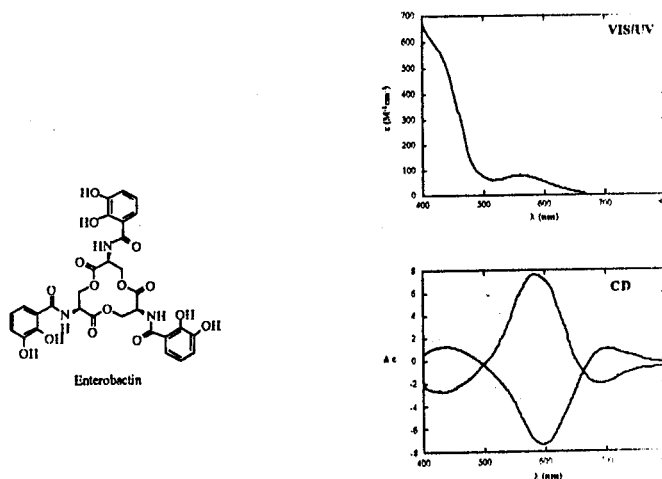


Fig. 4. The first use of CD and VIS/UV spectra to determine the chirality of a metal-siderophore complex: $[\text{Cr}^{\text{III}}(\text{enterobactin})]^{3-}$. VIS/UV spectrum (top) and CD spectrum (bottom) of $[\text{NH}_4]_3[\text{Cr}(\text{enterobactin})]$ (negative at 600 nm) and $\text{Cr}(\text{desferriferrichrome})$ (positive at 600 nm). (ref. 23).

Many studies have now shown that the primary recognition of the metal siderophore complex involves the metal coordination center and its chirality (ref. 4). A clear early example of that is shown by iron uptake mediated by rhodotorulic acid (Figure 5). Rhodotorulic acid is a dihydroxamic acid produced in relatively large amounts by the yeast *Rhodotorula pilimanae* (ref. 24). As noted earlier, ferrichrome is a tri-hydroxamic acid which forms a ferric complex with a preferred Λ (left-handed propeller) geometry at the metal center. Although *E. coli* does not produce ferrichrome, it has an active transport system that can recognize and transport this siderophore. Since rhodotorulic acid is a dihydroxamic acid, it accomplishes the full octahedral coordination of iron by making complexes that have a 3:2 ligand to metal stoichiometry. The absolute configuration at the metal center in these complexes is Δ , opposite to that in ferrichrome. Thus the mirror image enantiomer rhodotorulic acid (which was obtained by direct synthesis) must then have a preferred absolute configuration at the metal center which is Λ . As shown in Figure 5, it is the unnatural enantiomer rhodotorulic acid that was most effective in mediating iron uptake into *E. coli* (ref. 25). This is a consequence of the receptor protein recognizing preferentially the Λ absolute configuration for the tris-hydroxamate iron complex. That geometry only exists in the unnatural enantiomer rhodotorulic

and similar experiments represented a new kind of chiral recognition in biology: recognition of the chirality at an octahedral metal center rather than a chirality based on carbon.

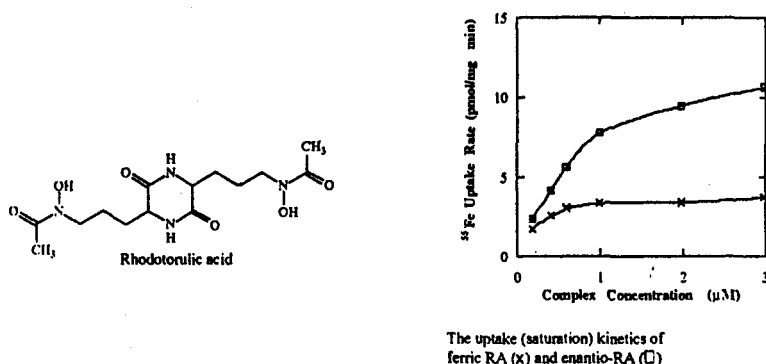


Fig. 5. The role of the stereochemistry at the metal center in siderophore recognition and transport. Shown is the uptake into *E. coli* of radioactive Fe as mediated by natural rhodotorulic acid versus its unnatural enantiomer (from ref. 25).

ENTEROBACTIN STRUCTURE AND Fe TRANSPORT

We will now focus exclusively on the siderophore enterobactin. Although this siderophore has now been known for almost 20 years, recent experimental results have finally explained two outstanding mysteries. Enterobactin is an extraordinarily powerful complexing agent, which is typical of the catecholate vs. hydroxamate siderophores (ref. 4). The genetics of its transport process has been thoroughly characterized, particularly by Professor Braun and coworkers (ref. 26), and will not be further reviewed here. Although there is a whole cascade of proteins now characterized in the outer membrane transport, only the *fepA* protein, which is involved in the initial recognition and transport of the complex, is shown in Figure 6. In the first application of Mössbauer spectroscopy to siderophore mediated iron transport (ref. 27) it was found that the enterobactin iron complex is taken up intact into the periplasmic region of the cell. *E. coli*, like other enteric bacteria, has two membranes, an outer and an inner (cytoplasmic) membrane. Although it was long thought in microbiology that the outer membrane only has a passive role in allowing molecular transport, there are now at least two examples, enterobactin mediated iron transport being one of them, where it is known that this is an active, energy-dependent, process (ref. 28).

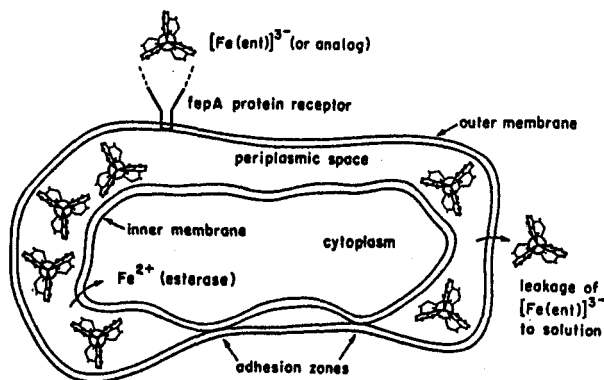


Fig. 6. The first use of Mössbauer spectroscopy to probe siderophore-mediated Fe transport into a living microbial cell. Shown is a schematic diagram of a cell of *E. coli*. The *fepA* outer membrane protein transports ferric enterobactin across a strong concentration gradient into the periplasmic space. Subsequent release of the iron, and destruction of the enterobactin, is a slower event (from ref. 27).

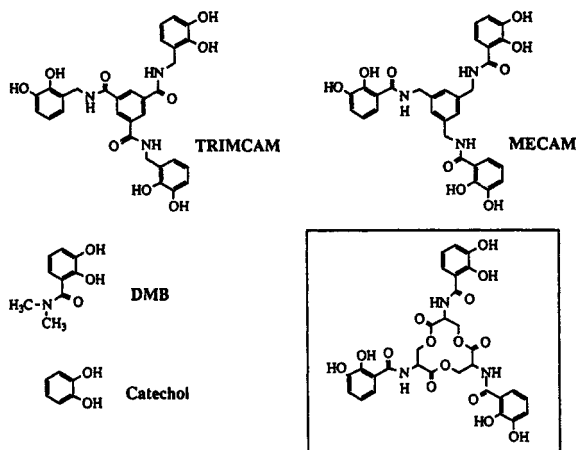
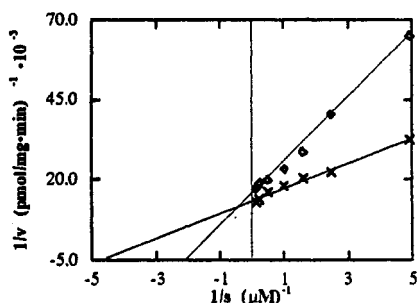


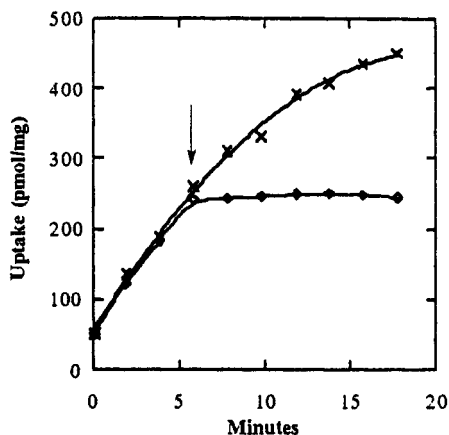
Fig. 7. Enterobactin analogs.

Synthetic analogs of enterobactin have been used to probe the iron uptake process. Several of these are shown in Figure 7. Shown at the lower right is enterobactin itself. The synthetic analogs, with their abbreviated names, are also shown in the figure. Transport studies, using metal complexes of these synthetic analogs, have been used to probe what aspects of the ferric enterobactin complex are recognized during the transport events. One example of this is shown in Figure 8. Iron uptake by enterobactin shows pseudo-enzyme kinetics (ref. 29). So-called double reciprocal plots then give



Substrate concentration (Lineweaver-Burk) plot of concentration-dependent uptake rates (pH 7.3). Symbols: $[^{55}\text{Fe}]$ enterobactin, (x); $[^{55}\text{Fe}]$ MECAM, (o).

Fig. 8. Iron uptake mediated by enterobactin and its synthetic analog MECAM. The quantitative comparison shows that both have the same limiting rate but that ferric enterobactin has an effective binding constant to the receptor protein that is about 3 times that of ferric MECAM (from ref. 29).



Inhibit of $2\ \mu\text{M}$ $^{55}\text{Fe}(\text{ent})$ uptake by $\text{Rh}(\text{DMB})_3^{3+}$. Control (x) represents uptake with no added inhibitor. $\text{K}_3[\text{Rh}(\text{DMB})_3]$ is added in 50 fold excess at 6 min (o).

Fig. 9. Transport of Fe uptake into *E. coli*, mediated by enterobactin. When the rhodium complex (enterobactin analog) is added it inhibits Fe uptake due to competitive binding to the protein receptor (from ref. 30).

straight lines and these in effect give the maximum rate of transport and the effective binding constant of the siderophore complex by the receptor protein. As can be seen, the maximum rate for iron uptake mediated by MECAM is the same as enterobactin, but the binding constant is somewhat lower. It was also shown that MECAM is an absolute inhibitor of iron uptake mediated by enterobactin — again showing that the MECAM analog is interacting with the same receptor that normally recognizes ferric enterobactin. Even simpler complexes could be used further to probe this process. In the case of the simple catechol rhodium(III) complexes, the kinetic inertness of the of the

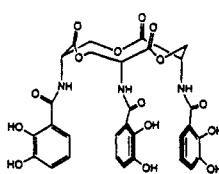
rhodium complex ensures that the tris catechol rhodium(III) complex remains intact during the transport experiment. Shown in Figure 9 is an example of the use of such a rhodium complex as an inhibitor. In one experiment the normal iron uptake mediated by enterobactin is shown as a function of time. In a second experiment a large excess of the rhodium complex is added at the point marked with an arrow, effectively shutting off further iron uptake mediated by enterobactin. This is characteristic of inhibition by competitive binding of the rhodium DMB complex at the metal site. In contrast (data not shown) the simple, unsubstituted rhodium catechol complex was not an inhibitor, showing that the carbonyl substitution on the catechol ring was an essential feature of the ferric enterobactin recognition process (ref. 30). Although early experiments had shown that the mirror image enantioenterobactin was not effective as a growth promoter (and by inference does not deliver iron to the microbial cell in a usable form) (ref. 31) recent experiments have shown that this is not because of the preferential recognition of the metal center chirality by the fep A protein (ref. 31). The difference in chirality must therefore be recognized later in the sequence of events that are shown in Figure 6.

ENTEROBACTIN - STRUCTURE AND STABILITY

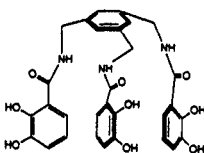
Although several synthetic analogs have been shown to be relatively effective in mimicking enterobactin, in every case they have been about a million fold weaker in their complexing ability. This is illustrated in Figure 10. Shown in this figure is both the formal stability constant (that is the formation of the metal complex from the fully deprotonated ligand) as well as the so-called pM value, which is a direct measure of the relative free energy under the conditions stated. For a total metal ion concentration of one micromolar and a total ligand concentration of 10 micromolar at physiological

	$\log K_f$	pM
Fe(ent) ³⁻	49	33.5
Fe(mecam) ³⁻	43	29.1
Fe(trencam) ³⁻	43	27.8

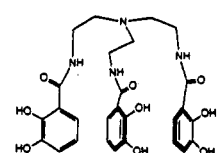
pM = $-\log[M]$
(pH=7.4 [M]=1 μ M; [L]=10 μ M)



Enterobactin



Mecam



Trencam

Fig. 10. The relative stability of enterobactin and model compounds (from ref. 33).

pH of 7.4, the negative log of the free ferric ion concentration (analogous to pH) is called pM. None of the synthetic analogs have been able to come close to the special stability of enterobactin (ref. 32). The origin of that stability is due to the triserine ring, since hydrolysis of one of the ester linkages (Figure 11) leads to a million fold reduction in the stability of the complex. Direct calorimetric studies (ref. 33) established the enthalpy of this process for both the intact enterobactin and the so-called linear enterobactin, the hydrolysis product shown in the figure. Since these reactions had to be carried out near neutral pH, it was the proton-dependent equilibrium shown in the figure that was measured, hence the difference in value relative to the normal stability constant. Nevertheless these stability constants for ferric enterobactin and ferric linear enterobactin (Figure 11) are directly comparable and show the six order of magnitude decrease of the enterobactin synthetic analogs. This free energy decrease is about 1/3 enthalpic and 2/3 entropic in origin. There has been a great deal of speculation about the origin of this special stability, but detailed structural information only recently has become available.

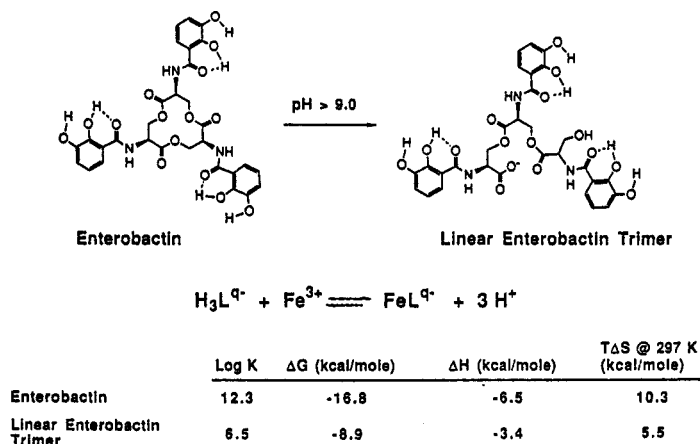
Thermodynamic Contributions to the Formation of Ferric Enterobactin

Fig. 11. The loss of stability of the ferric enterobactin complex due to hydrolysis of one ester bond of the ligand skeleton (from ref. 34).

The synthesis of the vanadium(IV) enterobactin complex gave for the first time usable crystals (ref. 34). The structure of the vanadium enterobactin complex anion is shown in Figure 12. Important structural features of the complex are also shown. It should be emphasized that the amide proton to catechol oxygen hydrogen bond is an important feature not only of the stability of the complex but, it is now believed, the rapid rate of formation of this complex. The crystal structure of enterobactin synthetic analogs have clearly shown that the neutral catechol ligands rotate around the carbon-carbon amide bond 180° so that the carbonyl oxygen hydrogen bonds with the protonated catechol in the neutral ligand. This structural change from the free ligand to the metal ligand complex involves only three degrees of freedom, as now can be seen from the structural information available.

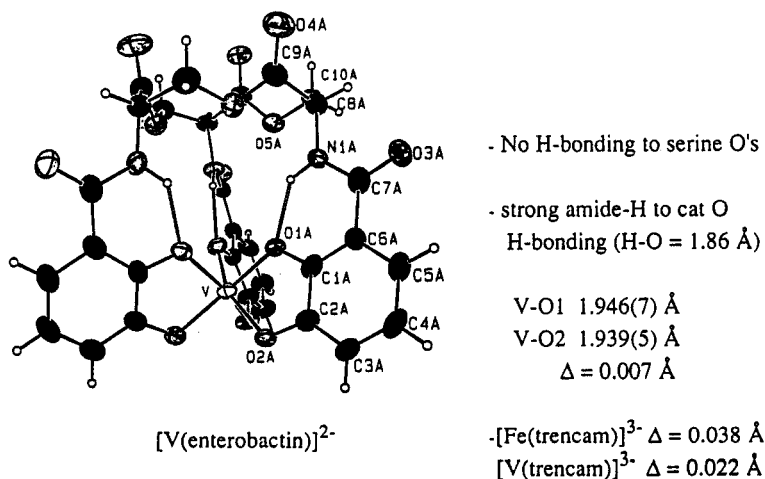


Fig. 12. The structure of the vanadium(IV) enterobactin complex (from ref. 35).

Shown in Figure 13 is the triserine backbone of enterobactin (with only the nitrogen substituent atoms shown) and, at right, a comparable trilactone synthesized some time ago by Shanzer and coworkers (ref. 35). When these two units are superimposed, a least squares fit shows that the largest atom deviations are on the order of 0.1 Å (ref. 34). In other words, the conformation of the triserine backbone of enterobactin is invariant with respect to coordination of the catechol groups. This imposes a fixed C-N vector for the amide linkages to the catechol groups and only one degree of freedom, rotation around this bond, is present for each catechol group. Hence the enterobactin molecule is predisposed for complexation (as opposed to preorganized, which would mean that the free ligand and metal ligand complex structures were essentially the same).

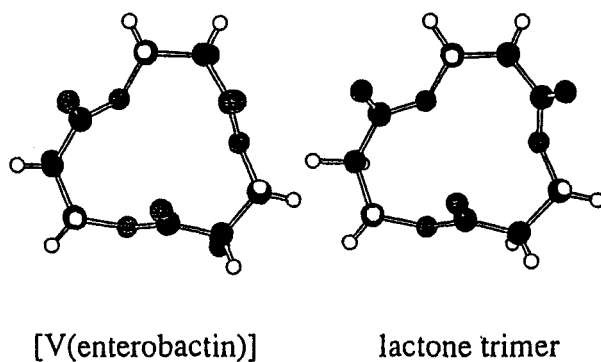


Fig. 13. A comparison of the skeleton of enterobactin and a synthetic trilactone by Shanzer et al. (from refs. 35 and 36).

A synthetic test of this hypothesis has recently been concluded with the synthesis of sterically encumbered enterobactin analogs (ref. 36). Shown in Figure 14 is another comparison of enterobactin and MECAM and substituted derivatives. By putting ethyl groups at the positions alternating with the catechol amide functionalities, an imposition of an up-down-up-down conformation is imposed which is very similar to the predisposition of the enterobactin structure. As a consequence there is a 10^4 increase in the stability of this substituted MECAM compared to the unsubstituted compound!

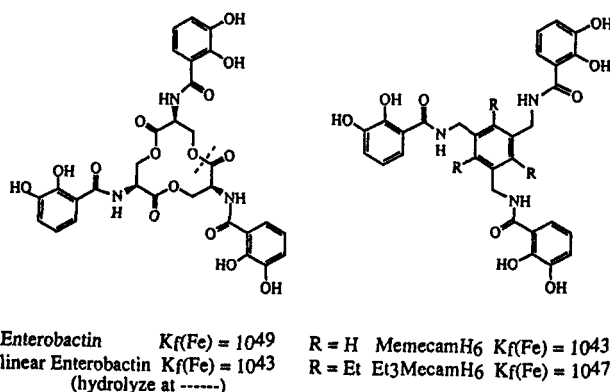


Fig. 14. A comparison of the stability of sterically hindered enterobactin analogs showing that enterobactin's special stability is due to its predisposition for metal binding caused by a decrease in the conformational degrees of freedom of the free ligand (from ref. 37)

CONCLUSION

Iron transport mediated by low-molecular-weight chelating agents (siderophores) has many practical applications. Our understanding of the important process of iron uptake by microbial cells is facilitated by understanding the fundamental coordination chemistry of the complexes and the bioorganic chemistry of the ligands. Synthetic analogs of the siderophores have been used to probe not just the biological transport process itself but also the structural and thermodynamic properties of these extraordinary ligands.

ACKNOWLEDGEMENT

I thank my many present and past coworkers who have been involved in this area of research and who are cited in the references. This work is supported by the National Institutes of Health through Grant AI11744. The assistance of Jason Telford in assembling this manuscript is gratefully acknowledged.

REFERENCES

1. J. W. Twort, G. L. Y. Ingram, Proc. Roy. Soc. Ser. B. Biol. Sci. **84**, 517 (1912).
2. G. A. Snow, J. Chem. Soc. , 4080 (1954).
3. G. A. Snow, Bacteriol. Rev. **34**, 99 (1970).
4. B. F. Matzanke, G. Müller-Matzanke, K. N. Raymond, in Physical Bioinorganic Chemistry Series, Iron Carriers and Iron Proteins. T. M. Loehr, Eds. (VCH Publishers, New York, 1989) pp. 1-121.
5. J. B. Neilands, et al., in Iron Transport in Microbes, Plants and Animals. F. Winkelmann, D. van der Helm, J. B. Neilands, Eds. (VCH Publishers, New York, 1987) pp. 3-33.
6. P. K. Bali, O. Zak, P. Aisen, Biochemistry **30**, 324-328 (1991).
7. K. Thorstensen, I. Romslo, Biochem. J. **271**, 1-10 (1990).
8. M. H. Kirking, Clinical Pharmacy **10**, 775-783 (1991).
9. M. J. Pippard, Acta Haemat. **78**, 206-211 (1987).
10. C. Borgna-Pignatti, A. Castriota-Scanderbeg, Haematologica **76**, 409-413 (1991).
11. L. Wolfe, et al., New England J. Med. **312**, 1600-1603 (1985).
12. R. Rolli, et al., Am. J. Physiol. **253**, 1372-1380 (1987).
13. L. A. Lee, et al., New England J. Med. **322**, 984-987 (1990).
14. H. C. Mofenson, T. R. Carraccio, N. Sharieff, New England J. Med. **316**, 1092-1093 (1987).
15. J. A. Stoebner, S. M. Payne, Infect. Immun. **56**, 2891 (1988).
16. C. Ratledge, in Iron Transport in Microbes, Plants and Animals. (VCH Publishers, New York, 1987) pp. 207-221.
17. D. E. ; R. Snider W. L., New Engl. J. Med. **326**, 703-705 (1992).
18. J. Leong, K. N. Raymond, J. Am. Chem. Soc. **96**, 6628-6630 (1974).
19. J. Leong, J. B. Neilands, K. N. Raymond, Biochem. Biophys. Res. Comm. **60**, 1066-1071 (1974).
20. T. B. Karpishin, M. S. Gebhard, E. I. Solomon, K. N. Raymond, J. Am. Chem. Soc. **113**, 2977-2984 (1991).
21. T. Emery, P. B. Hoffer, J. Nucl. Med. **21**, 935 (1980).
22. G. Müller, K. N. Raymond, J. Bacteriol. **160**, 304-312 (1984).
23. S. S. Isied, G. Kuo, K. N. Raymond, J. Am. Chem. Soc. **98**, 1763-1767 (1976).
24. C. J. Carrano, K. N. Raymond, J. Am. Chem. Soc. **100**, 5371-5374 (1978).
25. G. Müller, B. F. Matzanke, K. N. Raymond, J. Bacteriol. **160**, 313-318 (1984).
26. V. Braun, Biochem. Pept. Antibiot. **103**, 103-129 (1990).
27. B. Matzanke, et al., J. Bacteriol. **167**, 674-680 (1986).
28. V. Braun, K. Gunter, K. Hantke, Biol. Met. **4**, 14-22 (1991).
29. D. J. Ecker, B. Matzanke, K. N. Raymond, J. Bacteriol. **167**, 666-673 (1986).
30. D. J. Ecker, L. D. Loomis, M. E. Cass, K. N. Raymond, J. Am. Chem. Soc. **110**, 2457-2464 (1988).
31. J. B. Neilands, T. J. Erickson, W. H. Rastetter, J. Biol. Chem. **256**, 3831 (1981).
32. T. D. P. Stack, T. B. Karpishin, K. N. Raymond, J. Am. Chem. Soc. **114**, 1512-1514 (1992).
33. R. C. Scarrow, D. J. Ecker, C. Ng, S. Liu, K. N. Raymond, Inorg. Chem. **30**, 900-906 (1991).
34. T. B. Karpishin, T. M. Dewey, K. N. Raymond, J. Am. Chem. Soc. **115**, 1842-1851 (1993).
35. A. Shanzer, J. Libman, F. Frolow, J. Am. Chem. Soc. **103**, 7339 (1981).
36. T. D. P. Stack, Z. Hou, K. N. Raymond, J. Am. Chem. Soc. **115**, 0000 (1993).